



# ***OPN3* enhances the proliferation, migration, and invasion of triple-negative breast cancer cells via the regulation of the TGF- $\beta$ signaling pathway**

Yameng Liu<sup>1#</sup>, Yue Zhao<sup>2#</sup>, Jingjing Zhang<sup>1</sup>, Xiao Wu<sup>1</sup>, Yumei Li<sup>1</sup>, Ke Tang<sup>3</sup>, Zhengquan Han<sup>1</sup>

<sup>1</sup>Department of Medical Oncology, The First Affiliated Hospital of Bengbu Medical University, Bengbu, China; <sup>2</sup>Departments of Oncology Gynecology, The First Affiliated Hospital of Bengbu Medical University, Bengbu, China; <sup>3</sup>Department of Clinical Medicine, Bengbu Medical University, Bengbu, China

**Contributions:** (I) Conception and design: Y Liu, Y Zhao; (II) Administrative support: Y Li; (III) Provision of study materials or patients: J Zhang, X Wu, K Tang; (IV) Collection and assembly of data: Y Liu, Y Zhao, Z Han; (V) Data analysis and interpretation: Y Liu, Y Zhao; (VI) Manuscript writing: All authors; (VII) Final approval of manuscript: All authors.

<sup>#</sup>These authors contributed equally to this work as co-first authors.

**Correspondence to:** Dr. Zheng-quan Han, MM. Department of Medical Oncology, The First Affiliated Hospital of Bengbu Medical University, No. 287 Changhuai Road, Bengbu 233004, China. Email: hanzhengquan168@sina.com.

**Background:** *Opsin3* (*OPN3*) belongs to the guanine nucleotide-binding protein-coupled receptor superfamily, implicated in several pathological mechanisms that contribute to tumor development and resistance to treatment. This study examined *OPN3* expression in triple-negative breast cancer (TNBC) tissues and its function in TNBC cell propagation, invasion, and migration.

**Methods:** The study analyzed *OPN3* expression in TNBC patients and its diagnostic value using immunohistochemistry (IHC) staining and The Cancer Genome Atlas (TCGA) data. To evaluate the impact of *OPN3* on the growth, invasion, and migration of TNBC cells, both *in vitro* and *in vivo* experiments were carried out. The biological mechanisms of *OPN3*-induced cell migration and invasion were evaluated *via* quantitative real-time polymerase chain reaction (qRT-PCR) and Western blotting (WB) analyses.

**Results:** In this study, *OPN3* upregulation in TNBC tissues was found to be correlated with decreased overall survival (OS) and progression-free survival (PFS) rates. The propagation, invasion, and migration of BT-549 cells were promoted and apoptosis was reduced after *OPN3* overexpression. It was silenced in BT-549 cells, which resulted in the opposite effects. Further, the transforming growth factor-beta (TGF- $\beta$ )/SMAD2 signaling pathway was stimulated and the epithelial-mesenchymal transition (EMT) was modulated by *OPN3* overexpression in BT-549 cells.

**Conclusions:** The findings revealed that *OPN3* is involved in the stimulation of the TGF- $\beta$ /SMAD2 signaling pathway, which promotes the growth, migration, and dissemination of TNBC cells. Moreover, *OPN3* can serve as a diagnostic biomarker and a treatment target for TNBC.

**Keywords:** *OPN3*; triple-negative breast cancer (TNBC); TGF- $\beta$ /SMAD2 signaling pathway; migration and invasion; epithelial-mesenchymal transition (EMT)

Submitted Aug 06, 2024. Accepted for publication Dec 17, 2024. Published online Feb 26, 2025.

doi: 10.21037/tcr-24-1374

**View this article at:** <https://dx.doi.org/10.21037/tcr-24-1374>

## Introduction

Globally, breast cancer (BC) is a prevalent form of cancer that affects women. According to the Global Cancer Statistics 2022, it is responsible for 11.6% of all cancer cases and is the primary reason for cancer-related deaths among women (1). In specific, triple-negative breast cancer (TNBC) is a cause for concern due to the lack of the estrogen receptor (ER), progesterone receptor (PR), and human epidermal growth factor receptor 2 (HER2) (2,3). TNBC is the only subtype of BC that lacks targeted therapy and accounts for approximately 15–20% of newly diagnosed BCs. It is characterized by increased incidence rates, aggressiveness, elevated metastatic potential, and poor diagnostic outcomes due to its considerable molecular heterogeneity (4,5). Therefore, the investigation of possible therapeutic targets and prognostic predictive biomarkers is imperative to enhance the survival rates of individuals afflicted with TNBC.

The multifaceted stages involved in the process of metastasis are necessary to comprehend, as it is recognized as the primary contributor to almost all

types of cancer-related deaths. Multiple studies have depicted a substantial association between the invasive and metastatic characteristics of tumor cells and the epithelial-mesenchymal transition (EMT) (6-9). The cellular transformation of epithelial cells into mesenchymal cells is referred to as EMT. This process is distinguished by the loss of intercellular interactions, morphological changes from apical-basal to anterior-posterior polarity, and the formation of migratory mesenchymal cell properties (10). It is characterized by the substitution of E-calmodulin with N-calmodulin. A study has shown that EMT transcription factors (TFs), like Snail, Twist, and Zeb, play a crucial role in regulating the EMT process. They can suppress the gene expression related to the epithelial appearance while promoting the gene expression associated with the mesenchymal characteristics (11). Furthermore, another study also showed an association between the presence of mesenchymal traits in TNBC and the disease's heightened aggressiveness and propensity for tumor advancement (12).

*Opsin 3 (OPN3)* belongs to the G protein-coupled receptor superfamily and is situated on chromosome 1q43 (13-15). Research studies has shown that *OPN3* functions as an oncogene in tumor development. Particularly, a study indicates that *OPN3* may promote metastasis and EMT in lung adenocarcinoma (16). It has also been found that *OPN3* can affect apoptosis in hepatocellular carcinoma cells by altering the phosphorylation of Akt and Bcl2/bax, which in turn can influence the sensitivity of treatment (17). Furthermore, *OPN3* has been found to be related to the development and advancement of different types of tumors such as bladder uroepithelial carcinoma (BLCA), glioblastoma (GBM), low-grade glioma (LGG), gastric adenocarcinoma (STAD), and uveal melanoma (UVM), with its expression level showing a significant association with unfavorable outcomes in cancer patients (18). The role of *OPN3* in regulating melanogenesis and apoptosis in epidermal melanocytes has also been observed (19,20). Its overexpression has been found to be related to metastatic characteristics and a negative prognosis in limbal pigmented melanoma (21). However, limited data are available about the expression and functionality of *OPN3* in TNBC.

This study analyzed the gene expression profile of *OPN3* and examined its diagnostic importance in patients with TNBC. The impact of *OPN3* was also explored on TNBC cell propagation, dissemination, invasion, and its underlying molecular pathways were also elucidated. The study was mainly focused on providing novel perspectives into the progression of TNBC and identifying prognostic markers

### Highlight box

#### Key findings

- This study analyzed the gene expression profile of *Opsin3 (OPN3)* and examined its diagnostic importance in patients with triple-negative breast cancer (TNBC). The impact of *OPN3* was also explored on TNBC cell propagation, dissemination, invasion, and elucidation of its underlying molecular pathways. The study was mainly focused on providing novel perspectives into the progression of TNBC and identifying prognostic markers or therapeutic targets for TNBC patients.

#### What is known and what is new?

- Several studies have shown that *OPN3* plays a role as a pro-carcinogenic gene in tumours.
- In the present study, we found that the expression of *OPN3* was significantly elevated in TNBC tissues and correlated with poorer overall survival (OS) and progression-free survival (PFS) rates in patients. Furthermore, *OPN3* may play an important role in controlling the epithelial-mesenchymal transition (EMT) process in TNBC cells, in addition, the transforming growth factor-beta (TGF- $\beta$ )/SMAD2 pathway may be an important downstream of *OPN3*.

#### What is the implication, and what should change now?

- This study offers valuable biomarkers for accurately predicting the prognosis of TNBC, as well as their promising targets for developing effective treatments.

or therapeutic targets for TNBC patients. We present this article in accordance with the MDAR and ARRIVE reporting checklists (available at <https://tcr.amegroups.com/article/view/10.21037/tcr-24-1374/rc>).

## Methods

### Cell culture and transfection

Human BC cell lines (BT-549, SKBR-3, MDA-MB-231, MCF-7) and mammary normal epithelial cell line (HBL-100) were procured from Wuhan Punosai Biotechnology Co. (Wuhan, China). These cells were grown in RPMI-1640 medium enriched with fetal bovine serum (FBS) (10%) and Penicillin-Streptomycin-Amphotericin B Solution (1%) with 5% CO<sub>2</sub> at 37 °C.

*OPN3* siRNA (*siOPN3#1*: 5'-ACCUCCUCCUGGUCAACAUTT-3'; *siOPN3#2*: 5'-GUCACUUUACCUUCGUGUTT-3'; *siOPN3#3*: 5'-CAAUCCAAGUGAUAAGAUTT-3') and *OPN3* overexpression lentiviral vectors were acquired from GenePharma (Shanghai, China). BT-549 cells were maintained in 6-well plates and transfected when they reached the 80% confluence. Western blotting (WB) and quantitative real-time polymerase chain reaction (qRT-PCR) were conducted to validate the efficiency of transfection. LY2109761, a specific transforming growth factor-beta (TGF-β) receptor type I/II dual inhibitor (HY-12075), and TGF-β1 (HY-P700150AF) protein were obtained from MedChemExpress, Inc. (Shanghai, China).

### Immunohistochemistry (IHC) assay

Postoperative tumor tissues were collected from 44 TNBC patients who were surgically treated between January 2019 and June 2021 at the First Affiliated Hospital of Bengbu Medical University. The participants were all female, aged 28–78 years, with a mean age of 50.7 years. Standard procedures were implemented to conduct IHC analysis. Specifically, sections of tissue blocks from the 44 cases were deparaffinized, hydrated, and rinsed under running water. These specimens were stained with a diluted *OPN3* primary antibody (1:200, Affinity, Biosciences LTD, Jiangsu, China) and kept for 60 min at 20–25 °C, followed by dropwise addition of MaxVision™ HRP reagent (Fuzhou Meixin Co., Ltd., Fuzhou, China, KIT-5006). These tissue blocks were again incubated for 15 min at 20–25 °C and then processed with ethanol (dehydration), xylene (clearance),

hematoxylin (staining), and neutral gum (mounting). The IHC scores were independently reviewed by two competent pathologists. The study was conducted in accordance with the Declaration of Helsinki (as revised in 2013). The study procedure was approved by the respective ethics committee of Bengbu Medical University (approval No. 180.2022). All participants were informed *via* consent form before participation.

### RNA and qRT-PCR

The total content of RNA was isolated *via* RNA extraction solution (G3013-100ML; Wuhan Servicebio, Wuhan, China), followed by cDNA synthesis with the Nearshore Protein Reverse Transcription Kit (E047-01A) and detection *via* qRT-PCR using SYBR qPCR SuperMix Plus (E096-01A). The internal reference (control) gene was glyceraldehyde-3-phosphate dehydrogenase (*GAPDH*), and the  $\Delta\Delta C_t$  ( $2^{-\Delta\Delta C_t}$ ) method was applied to examine gene expression (fold change). The primers used are listed in Table S1. Three independent analyses of each biological sample were performed.

### Western blotting

Total cellular protein content was isolated *via* radio-immunoprecipitation assay (RIPA) lysis buffer (EpiZyme, Shanghai, China) and the concentration was estimated with the Omni-Easy™ Ready-to-Use BCA Protein Quantification Kit (EpiZyme: ZJ102). After isolation, protein samples (20–40 µg/lane) were loaded into 10% Sodium dodecyl sulfate polyacrylamide gel electrophoresis (SDS-PAGE) for protein separation and then transferred to a Polyvinylidene Fluoride (PVDF) membrane which was then kept with protein-free rapid containment solution (EpiZyme, PS108P) for 30 min at 20–25 °C. They were further kept for 24 h at 4 °C in the respective primary antibodies. The corresponding antibody dilutions (1:1,000) was prepared with *OPN3* (1:500, DF4877), E-cadherin (AF0131), N-cadherin (AF5239), Vimentin (AF7013), Snail (AF6023), p-SMAD2 (AF3449), total SMAD2 (AF6449), TGF-β1 (AF1027), or TGFBR1 (R044103150), and *GAPDH* (1:6,000, AF7021). The next day, the membranes were rinsed (thrice) and kept with HRP-linked goat anti-rabbit IgG (1:6,000, S0001) secondary antibody at 20–25 °C for 1 h. All antibodies were procured from Affinity Biosciences LTD and Wanlebio (Shenyang, China). Final protein bands were detected after incubation with an enhanced chemiluminescence reagent.

### ***Cell proliferation assay***

The effect of OPN3 on TNBC cell proliferation was assessed using a Cell Counting Kit-8 (CCK-8) (Apex Bio, Shanghai, China). Transfected BT-549 cells (3,000 cells/well) were cultured in 96-well plates. After incubation for 1, 2, 3, 4, and 5 days, 10  $\mu$ L of the CCK-8 assay solution was added to each well at the indicated time and incubated at 37 °C for 1–2 h. The assay was conducted in triplicate, and absorbances at 450 nm were measured in a Multiskan GO microplate reader (Thermo Fisher, USA).

### ***Colony formation assay***

The transfected BT-549 cells (700 cells/well) were cultured in 6-well culture plates at 37 °C with 5% CO<sub>2</sub>. During the incubation period, the medium was replaced every 3 days until clones containing more than 50 cells were observed. The plates were then washed 2–3 times with phosphate buffered saline (PBS) and fixed with 1 mL of 4% paraformaldehyde (PFA) per well for 15 min. After further washing, 1 mL of crystal violet staining solution (0.1%) was added to each well and incubated for 10 minutes. Finally, the entire 6-well plate was photographed and the number of clones was counted.

### ***Wound healing assay***

Transfected BT-549 cells were cultured ( $1.8 \times 10^5$  cells/well) into 6-well culture plates. The confluent (80–90%) monolayer of cells was scratched with a 200  $\mu$ L pipette tip. Afterward, the scratched area was washed thrice with PBS and maintained in a culture medium enriched with FBS (1%). Cell migration images were obtained at 0, 24, and 48 h post-scratch induction.

### ***Transwell assay***

This assay was conducted in two steps: (I) migration: culture medium with 20% FBS (600  $\mu$ L) was added to the lower chamber and basal medium (200  $\mu$ L) was added to the upper chamber containing transfected BT-549 cells ( $1.0 \times 10^4$  cells/200  $\mu$ L). (II) Invasion: Matrigel was thawed on ice, mixed with the basal medium (1:8), added 60  $\mu$ L to the upper chamber, and kept for 1–2 h. The liquid precipitated was discarded from the upper chamber, and the rest of the steps were the same as mentioned in the migration step. After spreading the plate, cells were kept

for 24 h at 37 °C. They were further proceeded by treating the cells, fixing with 4% PFA for 25 min, and staining with crystal violet (0.1%) for 15 min. Next, the staining solution was discarded, cells were washed and images were captured by selecting 5 different (random) fields under an inverted microscope.

### ***Apoptosis via flow cytometry***

An apoptosis assay was carried out using a commercially available kit (BestBio, Shanghai, China). Transfected BT-549 cells were grown in culture well plates and kept for 24 h. Cells were digested with EDTA-free trypsin, rinsed twice with PBS (chilled), suspended in 1X binding buffer (100  $\mu$ L), and stained with Annexin V-FITC/V-APC (5  $\mu$ L) and of PI (5  $\mu$ L) staining solutions. The cells were then kept for 8–10 min before adding 1X Binding buffer (400  $\mu$ L) and analyzing them using flow cytometry.

### ***Immunofluorescence***

Transfected BT-549 cells were allowed to grow ( $1 \times 10^5$  cells) on a 24 mm cell crawler. These cells were processed for fixation with PFA (4%), permeabilization with Triton X-100 (0.1%), and blocking with 5% BSA. The primary antibody was added for 24 h at 4 °C. Next, the cells were incubated with fluorescent secondary antibody for 2 h in dark conditions, followed by incubation with 4',6-diamidino-2-phenylindole dihydrochloride (DAPI) for 5 min.

### ***Enzyme-linked immunosorbent assay (ELISA)***

Transfected BT-549 cells were evenly distributed in culture well plates and kept for 24 h. The supernatant medium was collected and spun for 10 min at 1,000 rpm. The concentration of TGF- $\beta$ 1 was measured using the TGF- $\beta$ 1 kit provided by the manufacturer (SYP-H0688 UpingBio, Hangzhou, China) as per the manufacturer's instructions.

### ***Nude mouse tumor formation model***

SPF-grade female BALB/c-nu mice (4–6 weeks old, weight 18–20 g) were procured from Hangzhou Ziyuan Laboratory Animal Science and Technology Co. Ltd. (Hangzhou, China). In the axilla, the nude mice were then assigned to 2 groups (5 per group). Each group was inoculated with 100  $\mu$ L ( $5 \times 10^6$  cells) of cell suspension from either the BT-549 overexpression group or the BT-549 vector group.



Tumor size was recorded every 3–4 days with the following formula:  $\text{width}^2 \times \text{length} \times 0.5$ , to observe tumor growth. Mice were euthanized 22 days post-injection and their tumor tissues were then dissected, imaged, and weighed. A protocol was prepared before the study without registration. The animal studies were performed under a project license (No. 274.2022) granted by the ethics committee of Bengbu Medical University, in compliance with the national and institutional guidelines for the care and use of animals.

### Bioinformatics analysis

Multiple online resources were employed to analyze BC gene expression, such as GEPIA2.0 (<http://gepia2.cancer-pku.cn/#index>), bcGenExMiner v5.0 (<http://bcgenex.unicancer.fr/BC-GEM/GEM-requete.php>), and Sento Academic (<https://www.xiantaozi.com/?t=null>). In the “Baseline Data Sheet” module of the Xiantao academic website, the disease was selected as “Breast Cancer”, followed by selection of the first [The Cancer Genome Atlas-Breast invasive carcinoma (TCGA-BRCA)] TPM format dataset. The molecule was entered as “OPN3”, followed by the corresponding categorical and numerical variables, finally clicking Confirm. A survival analysis was conducted using the KMplot platform (<https://kmplot.com/analysis/>). Moreover, the GEPIA2.0 website and Timer2.0 (<http://timer.cistrome.org/>) were used to conduct a correlation analysis of OPN3 with E-cadherin, Vimentin, N-cadherin, Snail, TGFB1, and SMAD2.

### Statistical analyses

Data was statistically evaluated *via* SPSS software 25.0 V (IBM Corp, NY, USA) and GraphPad Prism 9.0. Each experiment was repeated thrice, and the data was depicted as the mean  $\pm$  standard deviation (SD). Groups were compared using a one-way analysis of variance (ANOVA) ( $\geq 2$  groups) or a two-tailed Student's *t*-test (2 groups). Correlations were evaluated using Pearson correlation analysis. Patients with different levels of OPN3 expression were examined using the chi-square test to determine their clinicopathological features. Survival curves were plotted *via* the Kaplan-Meier method. The univariate and multivariate survival analyses were carried out *via* the Cox proportional risk regression model. Two-sided  $P \leq 0.05$  was depicted as significant threshold.

## Results

### *Overexpression of OPN3 in TNBC tissues and cells related to unfavorable prognosis in TNBC patients*

To evaluate OPN3 expression in BC tissue, a comprehensive analysis was conducted using three online platforms (bcGenExMiner v5.0, Sento Academic, and GEPIA2.0). The results showed an elevated level of OPN3 expression in BC tissues relative to adjacent non-cancerous and normal tissues from the respective database. This increase is particularly prominent in TNBC tissues in contrast to other subtypes of BC (Figure 1A-1G). The analysis of the Kaplan-Meier method showed a considerable relationship between elevated OPN3 expression and reduced overall survival (OS) and recurrence-free survival (RFS) in patients (Figure 1H,1I). Consequently, the expression levels of OPN3 were evaluated in normal mammary epithelial cells HBL100, both TNBC cell lines (BT-549, MDA-MB-231), and non-TNBC cell lines (SKBR-3, MCF-7) *via* WB and qRT-PCR analyses (Figure 2A-2C). The findings revealed that the levels of OPN3 protein and mRNA were enhanced in BC cells as opposed to normal epithelial cells. Particularly, TNBC cells depicted overexpression than non-TNBC cells. These results were in line with the bioinformatics analysis. In BC tissues and cells, the expression of OPN3 was found to be significantly increased in TNBC relative to non-TNBC tissues and cells. This indicates a strong presence of OPN3 in BC, particularly in TNBC cases.

### *Overexpression of OPN3 reveals an unfavorable prediction of TNBC patients*

The study included approximately 44 TNBC patients, who underwent IHC staining of their cancer and adjacent paracancerous tissues to evaluate the levels of OPN3 expression. The findings depicted that OPN3 was substantially overexpressed in TNBC tissues as opposed to paracancerous tissues, as evidenced by the elevated IHC score detected in tumor tissues (Figure 2D,2E). A substantial connection was observed between OPN3 expression, Ki67 status ( $P=0.002$ ), and Pathologic TNM stage (TNM stage) ( $P=0.02$ ) in the clinicopathological analysis. However, no significant variations were found in other clinicopathological characteristics (Table 1). PFS was markedly related to lymph node (LN) metastasis ( $P=0.03$ ) and TNM staging ( $P=0.04$ ).

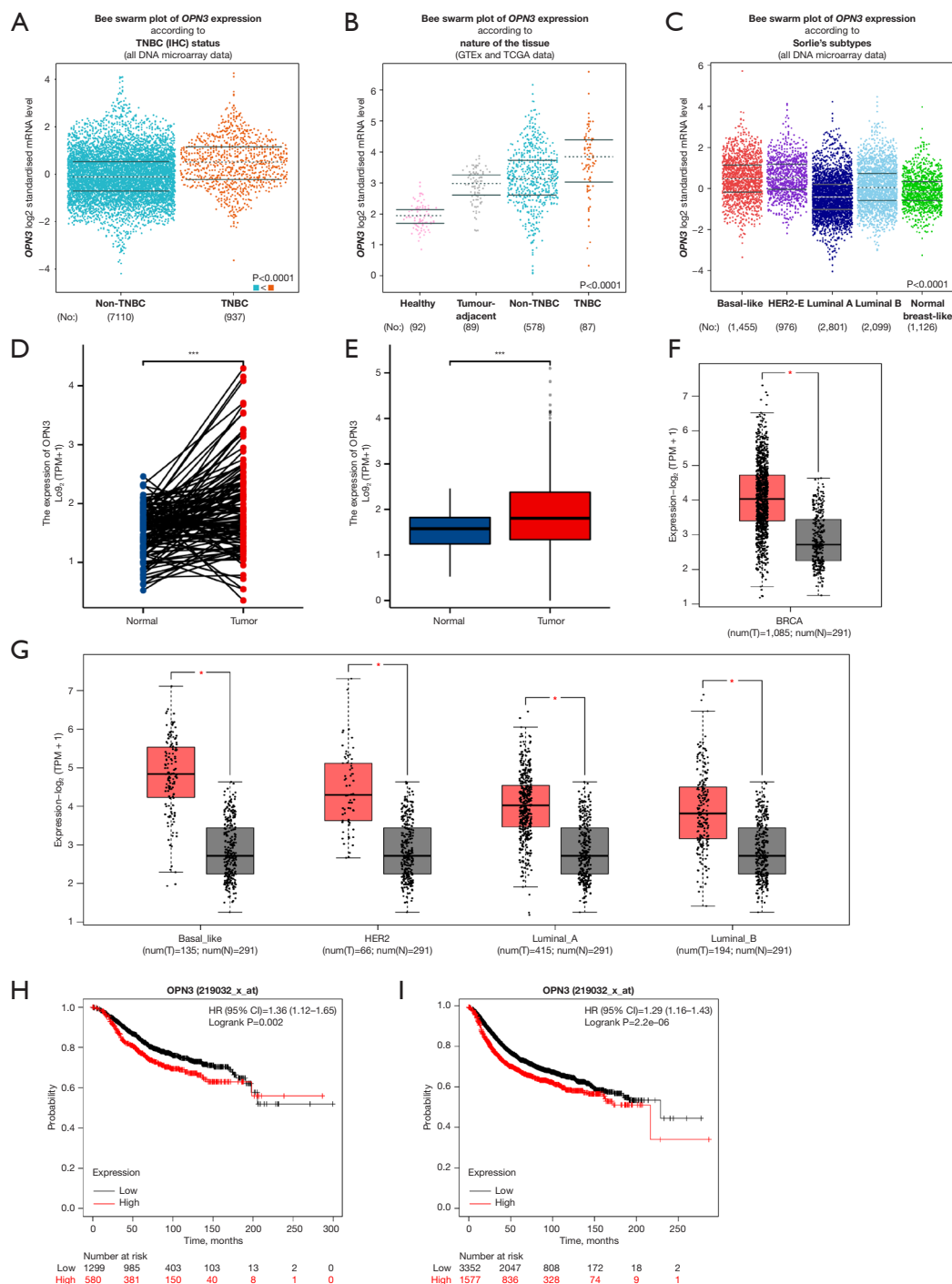


**Figure 1** Upregulation of *OPN3* in BC correlates with patient diagnosis in the TCGA database. (A-G) bcGenExMiner v5.0 (A-C), Sento academic (D,E), and GEPIA2.0 (F,G) databases depicting *OPN3* expression in TNBC, non-TNBC, and different BC subtypes, red represents tumor tissue, black represents normal tissue. (H,I) Kaplan-Meier Plotter online site plotted Kaplan-Meier plots for OS (H) and RFS (I) of BC patients based on *OPN3* expressions (high vs. low, log-rank test  $P = 0.002$ ,  $P \leq 0.001$ ). \*,  $P \leq 0.05$ ; \*\*\*,  $P \leq 0.001$ . *OPN3*, *Opsin3*; TNBC, triple-negative breast cancer; IHC, immunohistochemistry; BC, breast cancer; TCGA, The Cancer Genome Atlas; BRCA, breast invasive carcinoma; TPM, transcripts per million; HR, hazard ratio; CI, confidence interval; OS, overall survival; RFS, recurrence free survival.

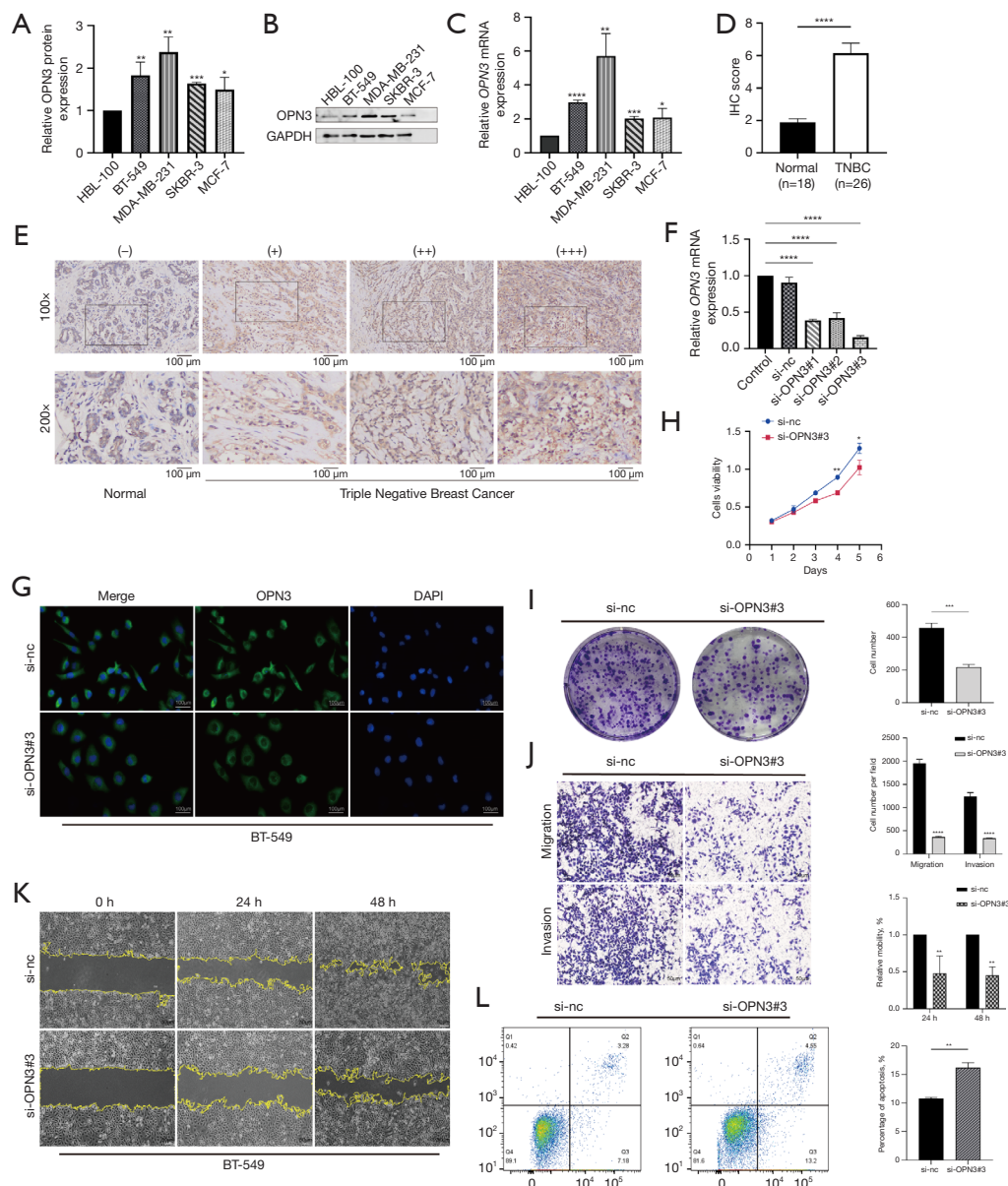


**Figure 2** Upregulation of OPN3 in TNBC cells and tissues correlates with the prognosis of patients, *OPN3* knockdown suppressed TNBC cell propagation, dissemination, and invasion and enhanced apoptosis *in vitro*. (A-C) Expression of *OPN3* in normal epithelial cells, TNBC, and non-TNBC cell proteins, and mRNAs was observed *via* WB and qRT-PCR. (D) Comparison of *OPN3* expression differences in TNBC and adjacent paracancerous tissues as per the IHC scores. (E) IHC representative plots of *OPN3* in TNBC tumor and adjacent paracancerous tissues (“-” represents negative “+” low, “++” moderate, “+++” high expressions). (F) *OPN3* level in BT-549 cells post-transfection with si-*OPN3* and si-nc *via* qRT-PCR analysis. (G) *OPN3* protein level was detected by immunofluorescence assay after transfection with si-*OPN3*#3 (50x). (H,I) Proliferative ability of BT-549 cells after suppression of *OPN3* was analyzed by CCK-8 and clone formation assay. (J,K) BT-549 cell invasive and migrating potential were evaluated through transwell and scratch assays after silencing of *OPN3* (100x). (L) Flow cytometry was employed to evaluate the apoptotic potential of BT-549 cells after the suppression of *OPN3*. Data are illustrated as mean  $\pm$  SD. \*,  $P \leq 0.05$ ; \*\*,  $P \leq 0.01$ ; \*\*\*,  $P \leq 0.001$ ; \*\*\*\*,  $P \leq 0.0001$  depicted as significant variations between groups. (I,J) Crystal violet staining method. *OPN3*, Opsin3; IHC, immunohistochemistry; TNBC, triple-negative breast cancer; WB, Western blotting; qRT-PCR, quantitative real-time polymerase chain reaction; CCK-8, Cell Counting Kit-8; DAPI, 4',6-diamidino-2-phenylindole dihydrochloride.

**Table 1** Clinicopathological features of TNBC patients and their associations with *OPN3* expression

Basic features	All patients (n=44), n (%)	High <i>OPN3</i> , n=26	Low <i>OPN3</i> , n=18	P value
Age at diagnosis (years)				0.17
≥45	28 (63.6)	17	15	
<45	16 (36.3)	9	3	
Lymphatic				0.11
N0	28 (63.6)	14	14	
N1–N3	16 (36.3)	12	4	
Ki67 status				0.002
≤20	18 (40.9)	11	16	
>20	26 (59.1)	15	2	
P53				0.65
–	13 (29.5)	7	6	
+	31 (70.4)	19	12	
TNM				0.02
I + II	33 (75.0)	16	17	
III + IV	11 (25.0)	10	1	

TNBC, triple-negative breast cancer; *OPN3*, Opsin3; TNM, pathologic TNM stage.

in univariate analysis among TNBC patients. Similarly, TNM staging ( $P=0.02$ ) demonstrated a prominent association with OS in TNBC patients. An independent predictive variable for PFS was identified as LN metastasis ( $P=0.02$ ) and TNM staging ( $P=0.008$ ) in a multifactorial Cox proportional risk model, while TNM stage ( $P=0.04$ ) was discovered as independently predictive variables for OS (Table 2). Moreover, TNBC patients were stratified into two groups for survival analysis, revealing that OS and PFS were substantially reduced in the subset with elevated *OPN3* expression compared to those with lower *OPN3* expression (Figure S1A,S1B). Furthermore, analysis of TCGA data indicated a significant relationship between high *OPN3* levels and both patient age and distant metastasis (Table S2). Collectively, these findings imply a strong association between increased *OPN3* expression and unfavorable outcomes in individuals with TNBC.

#### **Knockdown of *OPN3* inhibits TNBC cell propagation, invasion, and migration, and enhances apoptosis in vitro**

To analyze the functional significance of *OPN3* in TNBC cells, the BT-549 cell line was selected due to its moderate expression of *OPN3*. After transient transfection with si-

*OPN3*, the efficacy of interference was verified *via* qRT-PCR analysis, and si-*OPN3*#3 was selected for further analyses (Figure 2F). *OPN3* knockdown was further confirmed through immunofluorescence assays (Figure 2G). The CCK-8 and clone formation assays showed that suppression of *OPN3* markedly reduced the proliferative capacity of BT-549 cells (Figure 2H,2I). Moreover, the invasion and migration characteristics of BT-549 cells decreased as a result of *OPN3* suppression in both transwell and scratch assays (Figure 2J,2K). Flow analysis of apoptosis also indicated a significant increase in apoptotic cells within the si-*OPN3*#3 group as opposed to the si-nc group (Figure 2L), suggesting that the suppression of *OPN3* not only hindered proliferation, invasion, and migration but also promoted apoptosis in TNBC cells.

#### **Upregulation of *OPN3* enhanced in vitro and in vivo cell propagation, dissemination, and invasion, and suppressed apoptosis**

Similarly, lentiviral overexpression was also used to transfect the BT-549 cells. WB and qRT-PCR examinations revealed that the *OPN3* level was substantially upregulated in the lv-*OPN3* group as opposed to lv-nc (Figure 3A,3B).



**Table 2** Clinicopathologic factors for overall survival in all TNBC patients via univariate and multivariable analyses.

Variables	Univariate analysis				Multivariate analysis			
	PFS		OS		PFS		OS	
	HR (90% CI)	P value	HR (90% CI)	P value	HR (90% CI)	P value	HR (90% CI)	P value
OPN3 express (vs. high)								
Low	4.189 (0.503–6.856)	0.19	0.021 (0.002–3.826)	0.31				
Age (years) (vs. ≥45)								
<45	0.258 (0.061–1.094)	0.07	0.843 (0.071–0.856)	0.14				
Lymphatic (vs. N0)								
N1–N3	0.175 (0.335–0.873)	0.03	3.066 (0.511–4.398)	0.22	0.129 (0.024–0.695)	0.02		
Tumor grade (vs. I + II)								
III	0.335 (0.078–1.434)	0.14	3.762 (0.628–4.535)	0.15				
Ki67 status (vs. ≤20)								
>20	0.189 (0.038–0.938)	0.052	1.234 (0.092–3.334)	0.22				
P53 (vs. –)								
+	1.977 (0.441–8.868)	0.37	0.554 (0.092–3.334)	0.52				
TNM (vs. I + II)								
III + IV	0.212 (0.05–0.93)	0.04	2.857 (1.437–5.076)	0.02	0.118 (0.025–0.568)	0.008	3.074 (1.673–5.118)	0.04

A univariate Cox proportional hazard regression model was used to adjust the P value. TNBC, triple-negative breast cancer; PFS, progression-free survival; OS, overall survival; HR, hazard ratio; CI, confidence interval; *OPN3*, Opsin3; TNM, pathologic TNM stage.

Tumor formation assay in nude mice also showed that the propagation and tumor-forming potential of TNBC cells were enhanced by *OPN3* overexpression *in vivo* (Figure 3C–3E), while CCK-8 and colony formation assays confirmed that *OPN3* overexpression accelerated the propagation of BT549 cells (Figure 3F,3G). Transwell and scratch assays further showed that overexpression of *OPN3* promoted the invasive and migrating potential of BT549 cells. (Figure 3H,3I). Furthermore, the lv-*OPN3* group displayed a reduced number of apoptotic cells in contrast to the lv-nc group, as evidenced by the flow analysis of apoptosis (Figure 3J). This suggests that the *OPN3* overexpression markedly accelerated the propagation, invasion, and dissemination of TNBC cells, and simultaneously suppressed apoptosis.

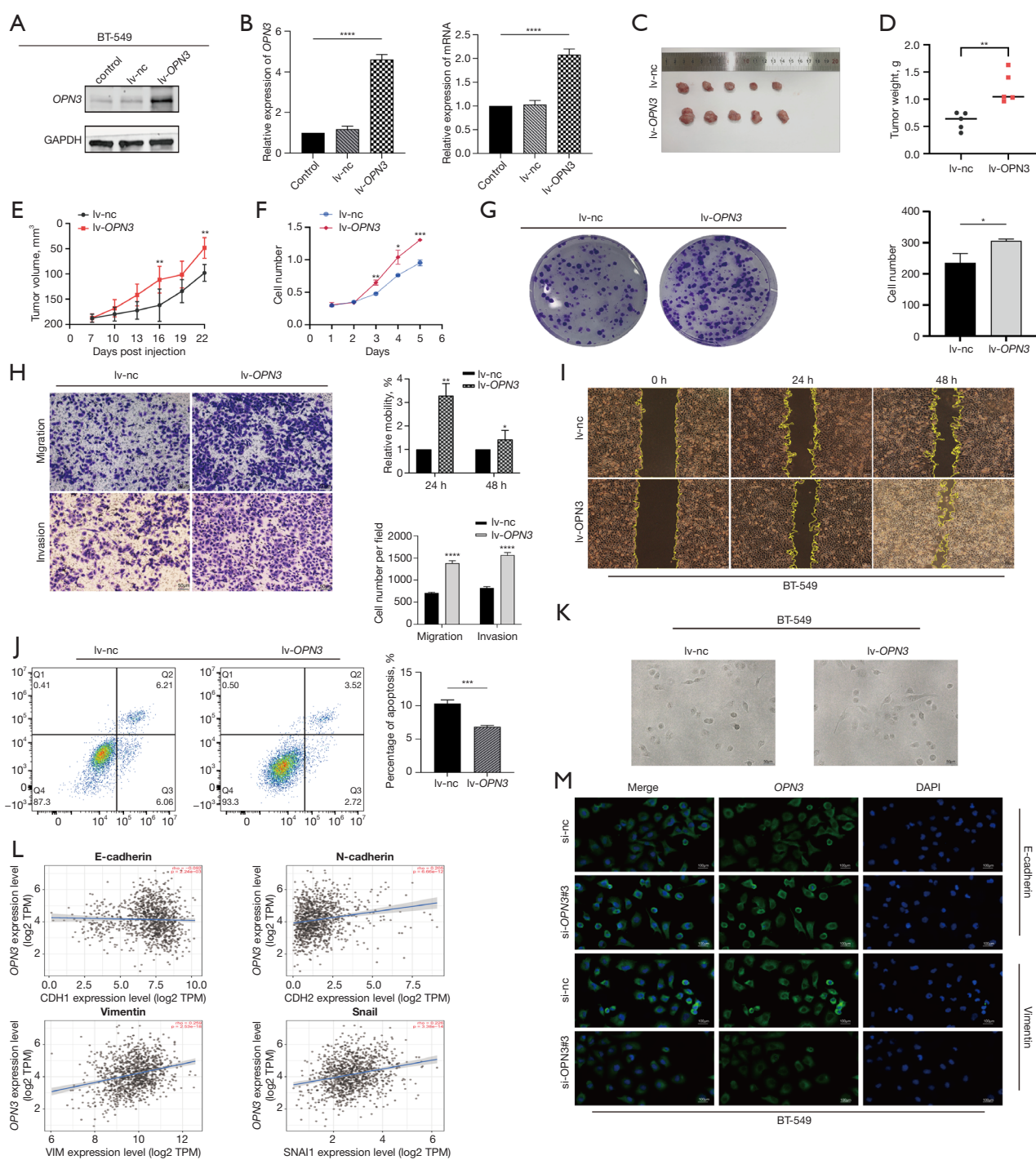
#### ***OPN3 can impact TNBC cell invasion and migration by affecting EMT***

The cells that were transfected with the vector maintained distinct margins, in contrast to those that displayed a spindle-shaped morphology post-*OPN3* overexpression,

as illustrated in Figure 3K. Further, bioinformatics analysis showed a negative association between *OPN3* expression and E-cadherin level, and a positive association with N-cadherin, Snail, and Vimentin levels (Figure 3L). Consequently, it was suggested that *OPN3* may influence tumor cell invasion and migration *via* the EMT process. Moreover, it was confirmed that the regulation of *OPN3* has the potential to influence the levels of EMT-associated mRNA and proteins *via* IF (Figure 3M), qRT-PCR (Figure 3N), and WB (Figure 3O,3P).

#### ***OPN3 induce EMT via the TGF-β/SMAD2 signaling pathway***

To further evaluate the mechanism by which *OPN3* influences EMT and the invasive and migratory traits of TNBC cells, the level of *OPN3* was strongly associated with the levels of TGFBR1 and SMAD2 in the TCGA database ( $P \leq 0.01$ , Figure 4A) using the GEPIA2.0 database. Based on the findings, ELISA was employed to identify the level of TGF-β1 in cells that either overexpressed or suppressed the levels of *OPN3*. The findings depicted that



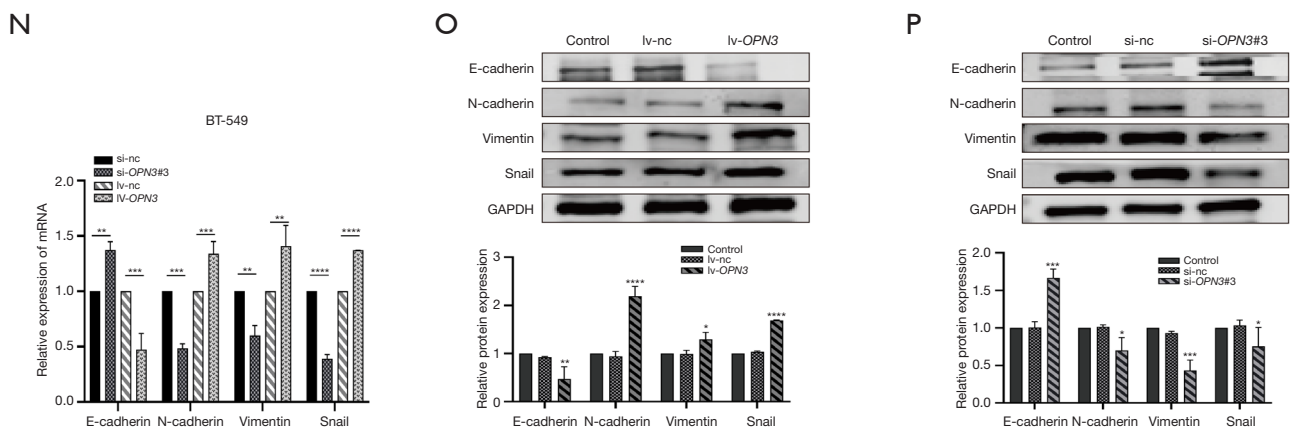


**Figure 3** *OPN3* overexpression enhances TNBC cell propagation, migration, and invasion *in vitro* and *in vivo*, and inhibits apoptosis, and *OPN3* enhances EMT in TNBC cells. (A,B) The expression pattern of *OPN3* in BT-549 cells post-transfection with lv-*OPN3* and lv-nc was analyzed *via* WB and qRT-PCR. (C-E) BT-549 cells were infected with lentiviral *OPN3* overexpression (lv-*OPN3*) or a control vector (lv-nc), and the BT-549 cells were injected (subcutaneous route) into female nude mice (N=5/group). (C) Images of tumor tissue 22 days after cell injection. (D) Measurement and comparison of tumor weights. (E) Changes in tumor volume were measured every three days after injection. (F,G) The impact of *OPN3* overexpression on the proliferative capacity of BT-549 cells was investigated by CCK-8 and clone formation. (H,I) Transwell and wound healing assays reveal the migration and invasive potential of BT-549 cells after *OPN3* overexpression (100×). (J) The apoptotic capacity of BT-549 cells after *OPN3* overexpression was examined by flow cytometry. (K) Cellular morphology changes after *OPN3* overexpression in BT-549 cells (400×). (L) The relationship between *OPN3* and E-cadherin, N-cadherin, Vimentin, and Snail is illustrated in Timer2.0. (M) Immunofluorescence images (50×) of the relationship between high and low expression of *OPN3* and EMT markers in BT-549 cells. (N) The expressions of mRNA of EMT-associated genes in BT-549 cells were analyzed *via* qRT-PCR to determine the effects of *OPN3* overexpression or suppression. (O,P) The expression patterns of EMT-related proteins in BT-549 cells with overexpression or silenced of *OPN3* were analyzed using WB. Data are illustrated as mean ± SD. \*,  $P \leq 0.05$ ; \*\*,  $P \leq 0.01$ ; \*\*\*,  $P \leq 0.001$ ; \*\*\*\*,  $P \leq 0.0001$  indicates substantial variations between groups. (G,H) Crystal violet staining method. *OPN3*, Opsin3; TNBC, triple-negative breast cancer; EMT, epithelial-mesenchymal transition; WB, Western blotting; qRT-PCR, quantitative real-time polymerase chain reaction; CCK-8, Cell Counting Kit-8; DAPI, 4',6-diamidino-2-phenylindole dihydrochloride.

the level of TGF- $\beta$ 1 was elevated in the supernatants of BT-549 cells overexpressing *OPN3*, while it was reduced in the supernatants with *OPN3* knockdown (Figure 4B). Furthermore, the levels of TGF- $\beta$ 1, TGFBR1, and P-SMAD2 were markedly raised by overexpression of *OPN3*, whereas the opposite result was found in knockdown *OPN3* in qRT-PCR analysis. Similarly, comparable results were observed in WB (Figure 4C,4D). This implies that the ectopic expression of *OPN3* may result in the transcription of TGF- $\beta$ 1 or its secretion, which eventually triggers the TGF- $\beta$  signaling pathway by raising the levels of TGF- $\beta$ 1 and TGFBR1. To further evaluate the mediating role of TGF- $\beta$ 1 in *OPN3*-induced EMT, TGF- $\beta$ 1 was used to stimulate the TGF- $\beta$ /SMAD2 pathway and LY2109761 to block the TGF- $\beta$ /SMAD2 pathway. The EMT phenotypes of BT-549 cells were all reversed to the vector level when overexpressed cells were exposed to LY2109761

(Figure S2A,S2B). LY2109761 inactivated the *OPN3*-mediated TGF- $\beta$ /SMAD2 pathway, whereas the knockdown of the *OPN3*-induced TGF- $\beta$ /SMAD2 pathway inactivation was reversed when BT-549 cells were treated with TGF- $\beta$ 1 (Figure 4E). Next, the propagation, invasion, and dissemination of TNBC cells were also observed. The analysis indicated that the TGF- $\beta$ /SMAD2 pathway was inhibited, resulting in a reduction in TNBC cell propagation, invasion, and migration in comparison to the lv-*OPN3* group. Conversely, the TGF- $\beta$ /SMAD2 pathway was activated, which accelerated TNBC cell propagation, invasion, and migration in comparison to the sh-*OPN3*#3 group (Figure 4F-4H). These findings represented that *OPN3* controlled the growth, invasion, and migration of TNBC cells via the TGF- $\beta$ /SMAD2-dependent pathway. Further, the TGF- $\beta$ /SMAD2 pathway may be a significant downstream signaling pathway of *OPN3* (Figure 5).



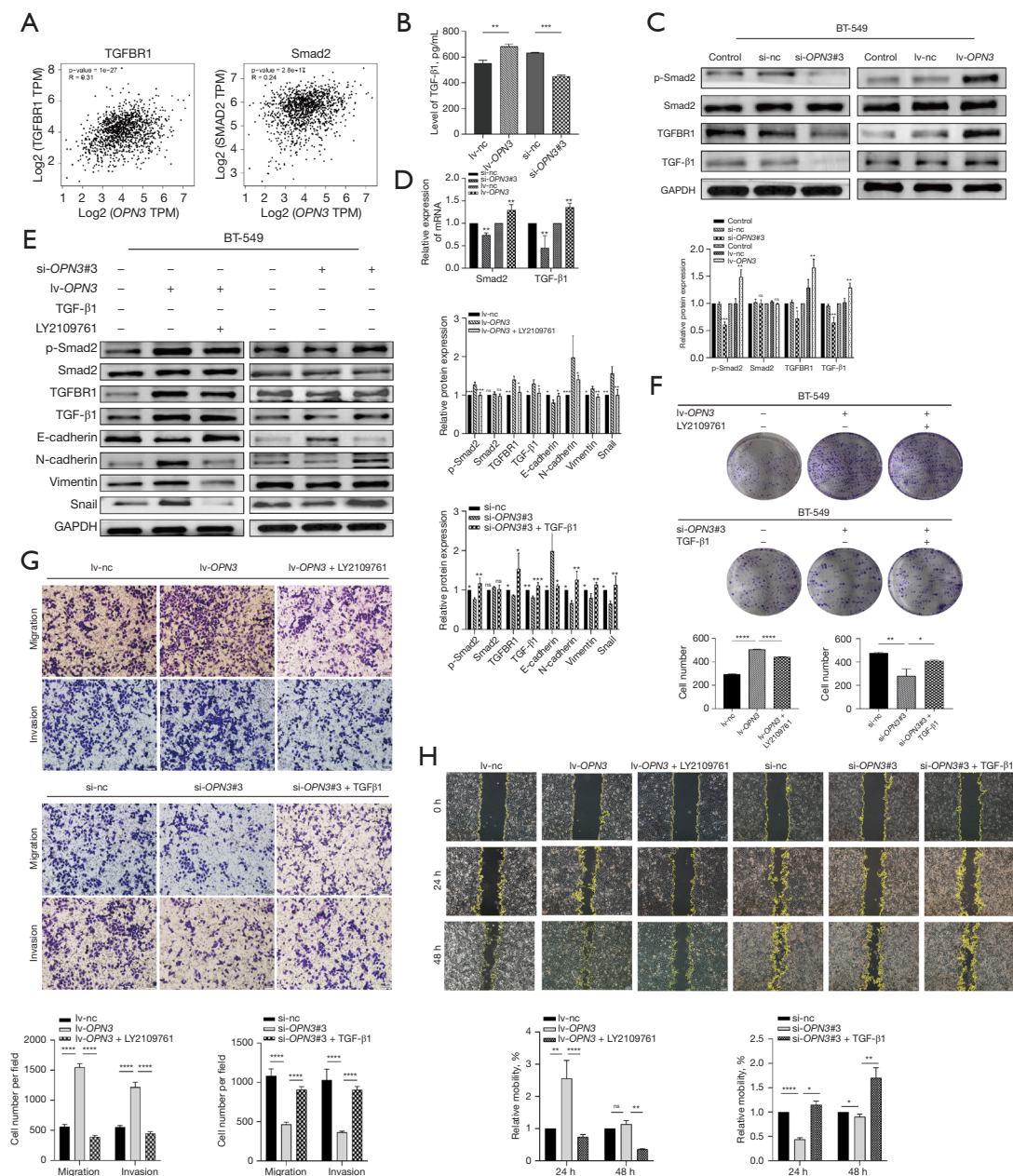


**Figure 4** *OPN3* enhances EMT *via* the TGF- $\beta$ /SMAD2 signaling pathway. (A) A positive association was observed between the levels of *OPN3* and those of *TGFBR1* and *SMAD2* in the GEPIA2.0 database analysis. (B) TGF- $\beta$  levels in the supernatants of BT-549 cells with either overexpression or silenced of *OPN3* were measured using ELISA. (C,D) The mRNA and protein levels of downstream proteins in the TGF- $\beta$  pathway were evaluated in BT-549 cells overexpressed or silenced *OPN3* using qRT-PCR and WB. (E) The levels of EMT-related and TGF- $\beta$  pathway downstream proteins in BT-549 cells treated with LY2109761 (1  $\mu$ mol) or TGF- $\beta$ 1 (10 ng/mL) following *OPN3* overexpression or silenced were examined by WB. (F) Clone formation assays were carried out to analyze the propagation of BT-549 cells after overexpression or silencing of *OPN3* with the addition of LY2109761 (1  $\mu$ mol) or TGF- $\beta$ 1 (10 ng/mL), respectively (100 $\times$ ). (G,H) Migrating and invasive potential of BT-549 cells were analyzed *via* transwell and scratch assays after the overexpression or silencing of *OPN3* with the addition of LY2109761 (1  $\mu$ mol) or TGF- $\beta$ 1 (10 ng/mL), respectively (100 $\times$ ). Data are illustrated as mean  $\pm$  SD. ns, not statistically significant; \*,  $P \leq 0.05$ ; \*\*,  $P \leq 0.01$ ; \*\*\*,  $P \leq 0.001$ ; \*\*\*\*,  $P \leq 0.0001$  indicates significant variations between groups. (F,G) Crystal violet staining method; *OPN3*, Opsin3; TGF- $\beta$ , transforming growth factor-beta; EMT, epithelial-mesenchymal transition; ELISA, enzyme-linked immunosorbent assay; WB, Western blotting; qRT-PCR, quantitative real-time polymerase chain reaction.



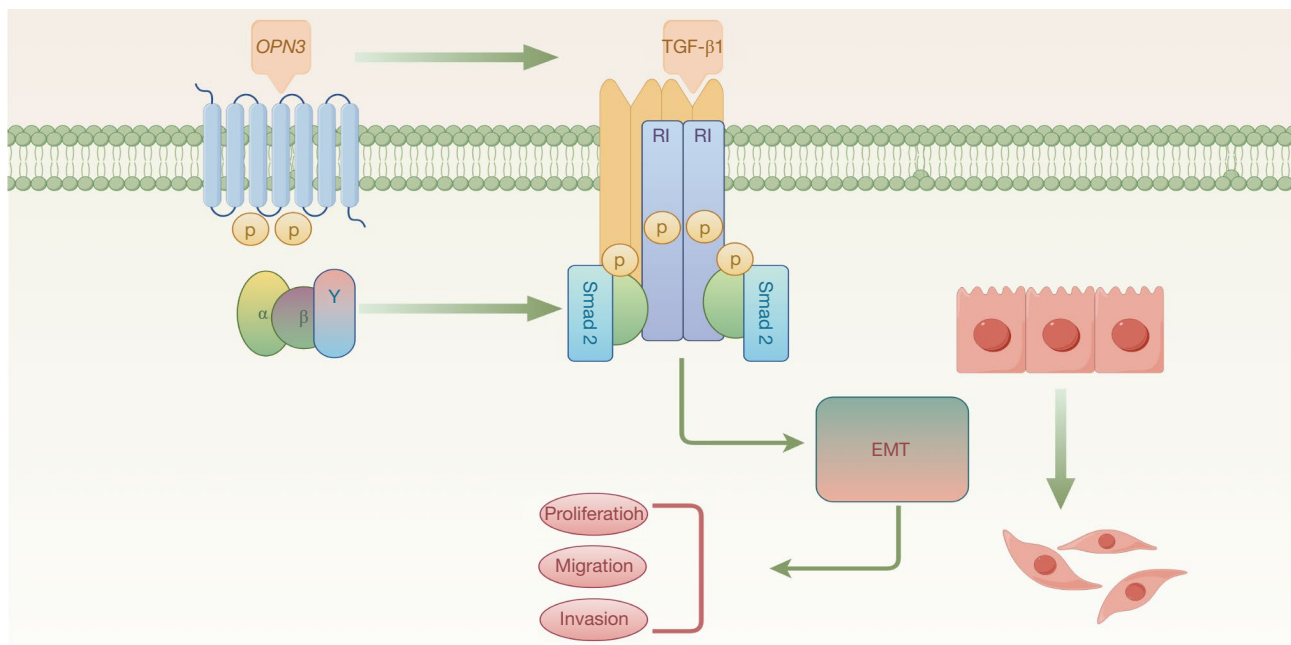


**Figure 5** Schematic diagram of *OPN3*-induced EMT model and promoting invasive metastasis of TNBC cells *via* TGF- $\beta$ /SMAD2 signaling pathway. This image was drawn from the Researcher's Home Online website, image export number: ID:UIPAI918b8. *OPN3*, Opsin3; EMT, epithelial-mesenchymal transition; TNBC, triple-negative breast cancer.

## Discussion

The emergence of novel treatment options is needed due to the high recurrence rates, strong metastatic potential, short OS, and lack of efficient targeted treatments that characterize TNBC, an aggressive subtype of BC (4,5). *OPN3* is a protein ubiquitously expressed in various human tissues, including the brain, epidermis, retina, liver, lungs, heart, and pancreas (13,22). Recently, there has been growing interest in the light-independent functions of *OPN3* in extraocular tissues, despite its classification as a photosensitive retinal protein. For instance, *OPN3* can negatively regulate melanin formation in human epidermal melanocytes by modulating the signaling of the melanocortin 1 receptor in a light-independent manner (19). It has been shown that downregulation of *OPN3* can induce melanocyte apoptosis *via* the mitochondrial apoptotic pathway (20). In lung cancer, *OPN3* can also promote EMT and lead to metastasis of lung adenocarcinoma (16). However, several studies have highlighted the significance of *OPN3* in the aggressive nature of malignant tumors, but its involvement in the occurrence and advancement of TNBC is still not explored. The current study revealed that the *OPN3* expression was substantially elevated in TNBC

tissues and was associated with poor OS and PFS rates in patients. This was the first time that this had been observed in this study. In contrast to normal breast epithelial cells, TNBC and HER2-enriched cell lines displayed enhanced *OPN3* protein and mRNA expression.

The process of metastasis involves multiple steps in which cancer cells infiltrate the surrounding tissue, enter the bloodstream, and establish secondary tumors in distant organs. Previous studies have indicated that TNBC frequently shows EMT molecular markers, which may contribute to its aggressive invasion and ability to spread to other parts of the body (23–26). Herein, a nude mouse tumorigenic model was developed to determine that the tumorigenic capacity of BT-549 cells was enhanced by the overexpression of *OPN3*. *In vitro* analysis demonstrated that the propagation, dissemination, and infiltration of TNBC cells were promoted by *OPN3* overexpression, whereas its suppression can suppress these characteristics of TNBC cells. In bioinformatics analysis, the *OPN3* expression revealed a negative relationship with E-cadherin and a positive relationship with N-cadherin, Vimentin, and Snail. This led to the suggestion that *OPN3* could potentially facilitate cell migration and invasion by influencing the level of EMT-associated genes. Western blotting and qRT-

PCR analyses also validated that the increased expression of *OPN3* led to an elevation in the levels of EMT-related markers like Vimentin, N-cadherin, and Snail. Conversely, the level of E-cadherin was found to be reduced. Contrary, the suppression of *OPN3* reversed this effect. These outcomes depicted that *OPN3* could play a significant role in controlling the EMT process in TNBC cells.

TGF- $\beta$  has several crucial roles in different cell processes such as cell propagation, infiltration, invasion, migration, EMT, extracellular matrix (ECM) remodeling, angiogenesis, and immunosuppression (27-29). Studies have demonstrated that TGF- $\beta$  signaling regulates tumorigenesis and cancer progression through a complex signaling network. In other types of cancers, TGF- $\beta$  is involved in multiple steps of metastasis, where the R-SMAD/coSMAD complex accumulates in the nucleus as a TF that promotes EMT after TGF $\beta$  stimulation (30,31). Moreover, several studies have shown that EMT in breast cells may be induced by TGF- $\beta$  and that this transformation leads to the acquisition of tumor-like characteristics by the cells (32,33). It is suggested that the TGF- $\beta$  pathway could have a considerable impact on the growth and metastasis of BC. Its suppression has shown promising results in improving the effectiveness of treatment and predicting outcomes for TNBC patients (34,35). Moreover, Wang *et al.* discovered that TGF- $\beta$ 2 can enhance tyrosinase activity in melanocytes *via* a mechanism involving *OPN3*, which is independent of the TGF- $\beta$ 2 receptor (36). In the supernatants of BT-549 cells, a positive relationship was observed between the levels of TGF- $\beta$ 1 and *OPN3* which predicted that *OPN3*-induced EMT was mediated by TGF- $\beta$  signaling. Next, BT-549 cells were stimulated with knockdown of *OPN3* using TGF- $\beta$ 1 and observed that the TGF- $\beta$ 1 protein effectively reversed the impact of *OPN3* knockdown on N-cadherin, Vimentin, p-SMAD2, and Snail. Moreover, TGF- $\beta$ 1 was able to counteract the increase in E-cadherin levels caused by *OPN3* knockdown. Similar results were obtained in BT-549 cells that overexpressed *OPN3* and were treated with the selective TGFBR1/II dual inhibitor LY2109761.

In this study, it was the first time reported, that the *OPN3* expression was increased in tissues and cells of TNBC and was related to OS and PFS in TNBC patients. However, the clinical data analysis did not yield any statistically significant results which may be attributed to the limited sample size used in this study. For future analyses, it may be necessary to include a larger sample size. While upregulation of *OPN3* was observed in HER2-enriched cell lines, these results require verification using a greater number of tissue samples

as well as in cell lines derived from different BC subtypes. In addition, it was noted that the stimulation of the TGF- $\beta$ /SMAD2 pathway may initiate *OPN3*-induced EMT in TNBC cells. It was also confirmed that the proliferative capacity of TNBC cells was enhanced by the overexpression of *OPN3*. However, the regulation of the TGF- $\beta$ /SMAD2 pathway and the specific targets of *OPN3* have not yet been elucidated, necessitating further research.

## Conclusions

This study concluded that *OPN3* is a significant indicator of unfavorable outcomes in TNBC. It was found that this gene has a crucial role in promoting EMT in TNBC cells through the stimulation of the TGF- $\beta$ /SMAD2 pathway, which leads to increased cell propagation, invasion, and dissemination. Therefore, this study offers valuable biomarkers for accurately predicting the prognosis of TNBC, as well as their promising targets for developing effective treatments.

## Acknowledgments

The authors would like to thank all the reviewers who participated in the review and MJEditor ([www.mjeditor.com](http://www.mjeditor.com)) for its linguistic assistance during the preparation of this manuscript.

## Footnote

**Reporting Checklist:** The authors have completed the MDAR and ARRIVE reporting checklists. Available at <https://tcr.amegroups.com/article/view/10.21037/tcr-24-1374/rc>

**Data Sharing Statement:** Available at <https://tcr.amegroups.com/article/view/10.21037/tcr-24-1374/dss>

**Peer Review File:** Available at <https://tcr.amegroups.com/article/view/10.21037/tcr-24-1374/prf>

**Funding:** This study was supported by the Natural Science Fund for Colleges and Universities of Anhui Province (No. KJ2021A0703).

**Conflicts of Interest:** All authors have completed the ICMJE uniform disclosure form (available at <https://tcr.amegroups.com/article/view/10.21037/tcr-24-1374/coif>). The authors have no conflicts of interest to declare.

**Ethical Statement:** The authors are accountable for all aspects of the work in ensuring that questions related to the accuracy or integrity of any part of the work are appropriately investigated and resolved. The study was conducted in accordance with the Declaration of Helsinki (as revised in 2013). The study procedure was approved by the respective ethics committee of Bengbu Medical University (No. 180.2022). All participants were informed via consent form before participation. The animal studies were performed under a project license (No. 274.2022) granted by the ethics committee of Bengbu Medical University, in compliance with the national and institutional guidelines for the care and use of animals.

**Open Access Statement:** This is an Open Access article distributed in accordance with the Creative Commons Attribution-NonCommercial-NoDerivs 4.0 International License (CC BY-NC-ND 4.0), which permits the non-commercial replication and distribution of the article with the strict proviso that no changes or edits are made and the original work is properly cited (including links to both the formal publication through the relevant DOI and the license). See: <https://creativecommons.org/licenses/by-nc-nd/4.0/>.

## References

- Bray F, Laversanne M, Sung H, et al. Global cancer statistics 2022: GLOBOCAN estimates of incidence and mortality worldwide for 36 cancers in 185 countries. *CA Cancer J Clin* 2024;74:229-63.
- Brenton JD, Carey LA, Ahmed AA, et al. Molecular classification and molecular forecasting of breast cancer: ready for clinical application? *J Clin Oncol* 2005;23:7350-60.
- Yang R, Li Y, Wang H, et al. Therapeutic progress and challenges for triple negative breast cancer: targeted therapy and immunotherapy. *Mol Biomed* 2022;3:8.
- Zagami P, Carey LA. Triple negative breast cancer: Pitfalls and progress. *NPJ Breast Cancer* 2022;8:95.
- Chang-Qing Y, Jie L, Shi-Qi Z, et al. Recent treatment progress of triple negative breast cancer. *Prog Biophys Mol Biol* 2020;151:40-53.
- Aiello NM, Kang Y. Context-dependent EMT programs in cancer metastasis. *J Exp Med* 2019;216:1016-26.
- Yeung KT, Yang J. Epithelial-mesenchymal transition in tumor metastasis. *Mol Oncol* 2017;11:28-39.
- Pastushenko I, Blanpain C. EMT Transition States during Tumor Progression and Metastasis. *Trends Cell Biol* 2019;29:212-26.
- Pei D, Shu X, Gassama-Diagne A, et al. Mesenchymal-epithelial transition in development and reprogramming. *Nat Cell Biol* 2019;21:44-53.
- Ye X, Weinberg RA. Epithelial-Mesenchymal Plasticity: A Central Regulator of Cancer Progression. *Trends Cell Biol* 2015;25:675-86.
- Nieto MA, Huang RY, Jackson RA, et al. EMT: 2016. *Cell* 2016;166:21-45.
- Grasset EM, Dunworth M, Sharma G, et al. Triple-negative breast cancer metastasis involves complex epithelial-mesenchymal transition dynamics and requires vimentin. *Sci Transl Med* 2022;14:eabn7571.
- Halford S, Freedman MS, Bellingham J, et al. Characterization of a novel human opsin gene with wide tissue expression and identification of embedded and flanking genes on chromosome 1q43. *Genomics* 2001;72:203-8.
- Sato M, Tsuji T, Yang K, et al. Cell-autonomous light sensitivity via Opsin3 regulates fuel utilization in brown adipocytes. *PLoS Biol* 2020;18:e3000630.
- Andrabi M, Upton BA, Lang RA, et al. An Expanding Role for Nonvisual Opsins in Extraocular Light Sensing Physiology. *Annu Rev Vis Sci* 2023;9:245-67.
- Xu C, Wang R, Yang Y, et al. Expression of OPN3 in lung adenocarcinoma promotes epithelial-mesenchymal transition and tumor metastasis. *Thorac Cancer* 2020;11:286-94.
- Jiao J, Hong S, Zhang J, et al. Opsin3 sensitizes hepatocellular carcinoma cells to 5-fluorouracil treatment by regulating the apoptotic pathway. *Cancer Lett* 2012;320:96-103.
- Zhang W, Feng J, Zeng W, et al. Integrated analysis of the prognostic and oncogenic roles of OPN3 in human cancers. *BMC Cancer* 2022;22:187.
- Ozdeslik RN, Olinski LE, Trieu MM, et al. Human nonvisual opsin 3 regulates pigmentation of epidermal melanocytes through functional interaction with melanocortin 1 receptor. *Proc Natl Acad Sci U S A* 2019;116:11508-17.
- Wang Y, Lan YH, Lu HG. Opsin3 Downregulation induces apoptosis of Human epidermal melanocytes via mitochondrial pathway. *Photochem Photobiol* 2020;96:83-93.
- Zeng W, Zhang W, Feng J, et al. Expression of OPN3 in acral lentiginous melanoma and its associated with clinicohistopathologic features and prognosis. *Immun Inflamm Dis* 2021;9:840-50.

22. Haltaufderhyde K, Ozdeslik RN, Wicks NL, et al. Opsin expression in human epidermal skin. *Photochem Photobiol* 2015;91:117-23.
23. Löönd F, Sugiyama N, Bill R, et al. Distinct contributions of partial and full EMT to breast cancer malignancy. *Dev Cell* 2021;56:3203-3221.e11.
24. Garrido-Castro AC, Lin NU, Polyak K. Insights into Molecular Classifications of Triple-Negative Breast Cancer: Improving Patient Selection for Treatment. *Cancer Discov* 2019;9:176-98.
25. Jang MH, Kim HJ, Kim EJ, et al. Expression of epithelial-mesenchymal transition-related markers in triple-negative breast cancer: ZEB1 as a potential biomarker for poor clinical outcome. *Hum Pathol* 2015;46:1267-74.
26. Cheung SY, Boey YJ, Koh VC, et al. Role of epithelial-mesenchymal transition markers in triple-negative breast cancer. *Breast Cancer Res Treat* 2015;152:489-98.
27. Wang X, Eichhorn PJA, Thiery JP. TGF- $\beta$ , EMT, and resistance to anti-cancer treatment. *Semin Cancer Biol* 2023;97:1-11.
28. Shi X, Yang J, Deng S, et al. TGF- $\beta$  signaling in the tumor metabolic microenvironment and targeted therapies. *J Hematol Oncol* 2022;15:135.
29. Battle E, Massagué J. Transforming Growth Factor- $\beta$  Signaling in Immunity and Cancer. *Immunity* 2019;50:924-40.
30. Yang H, Wang L, Zhao J, et al. TGF- $\beta$ -activated SMAD3/4 complex transcriptionally upregulates N-cadherin expression in non-small cell lung cancer. *Lung Cancer* 2015;87:249-57.
31. Tong X, Wang S, Lei Z, et al. MYOCD and SMAD3/SMAD4 form a positive feedback loop and drive TGF- $\beta$ -induced epithelial-mesenchymal transition in non-small cell lung cancer. *Oncogene* 2020;39:2890-904.
32. Shukla N, Naik A, Moryani K, et al. TGF- $\beta$  at the crossroads of multiple prognosis in breast cancer, and beyond. *Life Sci* 2022;310:121011.
33. Yi M, Wu Y, Niu M, et al. Anti-TGF- $\beta$ /PD-L1 bispecific antibody promotes T cell infiltration and exhibits enhanced antitumor activity in triple-negative breast cancer. *J Immunother Cancer* 2022;10:e005543.
34. Panagi M, Voutouri C, Mpekris F, et al. TGF- $\beta$  inhibition combined with cytotoxic nanomedicine normalizes triple negative breast cancer microenvironment towards anti-tumor immunity. *Theranostics* 2020;10:1910-22.
35. Zhang J, Zhang Z, Huang Z, et al. Isoosendanin exerts inhibition on triple-negative breast cancer through abrogating TGF- $\beta$ -induced epithelial-mesenchymal transition via directly targeting TGF $\beta$ R1. *Acta Pharm Sin B* 2023;13:2990-3007.
36. Wang Y, Lan Y, Yang X, et al. TGF $\beta$ 2 Upregulates Tyrosinase Activity through Opsin-3 in Human Skin Melanocytes In Vitro. *J Invest Dermatol* 2021;141:2679-89.

**Cite this article as:** Liu Y, Zhao Y, Zhang J, Wu X, Li Y, Tang K, Han Z. OPN3 enhances the proliferation, migration, and invasion of triple-negative breast cancer cells via the regulation of the TGF- $\beta$  signaling pathway. *Transl Cancer Res* 2025;14(2):1141-1156. doi: 10.21037/tcr-24-1374